J|A|C|S
ARTICLES
Published on Web 05/09/2007

Dynamical Regulation of Ligand Migration by a Gate-Opening Molecular Switch in Truncated Hemoglobin-N from *Mycobacterium tuberculosis*

Axel Bidon-Chanal,[†] Marcelo A. Martí,[‡] Darío A. Estrin*,[‡] and F. Javier Luque*,[†]

Contribution from the Departament de Fisicoquímica, Facultat de Farmàcia, Universitat de Barcelona, Avenida Diagonal 643, 08028, Barcelona, Spain, and Departamento de Química Inorgánica, Analítica y Química Física/INQUIMAE-CONICET, Facultad de Ciencias Exactas y Naturales, Universidad de Buenos Aires, Ciudad Universitaria, Pabellón 2, Buenos Aires, C1428EHA, Argentina

Received December 15, 2006; E-mail: fjluque@ub.es; dario@qi.fcen.uba.ar

Abstract: Truncated hemoglobin-N is believed to constitute a defense mechanism of *Mycobacterium tuberculosis* against NO produced by macrophages, which is converted to the harmless nitrate anion. This process is catalyzed very efficiently, as the enzyme activity is limited by ligand diffusion. By using extended molecular dynamics simulations we explore the mechanism that regulates ligand diffusion and, particularly, the role played by residues that assist binding of O_2 to the heme group. Our data strongly support the hypothesis that the access of NO to the heme cavity is dynamically regulated by the TyrB10−GlnE11 pair, which acts as a molecular switch that controls opening of the ligand diffusion tunnel. Binding of O_2 to the heme group triggers local conformational changes in the TyrB10−GlnE11 pair, which favor opening of the PheE15 gate residue through global changes in the essential motions of the protein skeleton. The complex pattern of conformational changes triggered upon O_2 binding is drastically altered in the GlnE11→Ala and TyrB10→Phe mutants, which justifies the poor enzymatic activity observed experimentally for the TyrB10→Phe form. The results support a molecular mechanism evolved to ensure access of NO to the heme cavity in the oxygenated form of the protein, which should warrant survival of the microorganism under stress conditions.

Introduction

Globins are found in all kingdoms of living organisms. Besides their function in assisting O_2 transport and storage, novel functions have been identified in the last years, such as control of nitric oxide (NO) levels in microorganisms. In *Mycobacterium tuberculosis*, which infects about one-third of the human population and causes more than a million deaths per year,[1] the NO resistance is based on the NO-dioxygenase activity of the oxygenated form of truncated hemoglobin-N (trHbN), which converts NO into nitrate anion,[2−4] thus contributing to induction and maintenance of bacilli latency.[5,6]

Truncated hemoglobins make up a distinct group within the hemoglobin superfamily.[7] Their tertiary structure consists of a 2-on-2 helical sandwich, which is a subset of the 3-on-3 sandwich of the classical globin fold.[8] Despite their small size, several truncated hemoglobins host an apolar tunnel that connects the heme pocket with the protein surface.[9−11] In trHbN from *M. tuberculosis* the tunnel system is built by two perpendicular branches of about 8 and 20 Å length, which differ from the cavities observed in sperm whale myoglobin. Moreover, it has been hypothesized to control diatomic ligand migration to the heme, which would be the rate-limiting step in NO conversion to nitrate.[2,3]

The role played by the ligand migration tunnel in trHbN has been explored by means of extended molecular dynamics (MD) simulations of both deoxygenated and oxygenated forms of trHbN, which have unraveled a dual-path ligand-induced regulation mechanism underlying diffusion of both O_2 and NO in trHbN.[12,13] According to this mechanism, ligand migration

[†] Universitat de Barcelona.
[‡] Universidad de Buenos Aires.

(1) Bloom, B. R. *Tuberculosis: Pathogenesis, Protection and Control*; ASM Press: Washington D.C., 1994.
(2) Ouellet, H.; Ouellet, Y.; Richard, C.; Labarre, M.; Wittenberg, B.; Wittenberg, J.; Guertin, M. *Proc. Natl. Acad. Sci. U.S.A.* **2002**, *99*, 5902.
(3) Couture, M.; Yeh, S. R.; Wittenberg, B. A.; Wittenberg, J. B.; Ouellet, Y.; Rousseau, D. L.; Guertin, M. *Proc. Natl. Acad. Sci. U.S.A.* **1999**, *96*, 11223.
(4) Pathania, R.; Navani, N. K.; Gardner, A. M.; Gardner, P. R.; Dikshit, K. L. *Mol. Microbiol.* **2002**, *45*, 1303.
(5) MacMicking, J. D.; North, R. J.; LaCourse, R.; Mudgett, J. S.; Shah, S. K.; Nathan, C. F. *Proc. Natl. Acad. Sci. U.S.A.* **1997**, *94*, 5243.
(6) Shiloh, M. U.; Nathan, C. F. *Curr. Opin. Microbiol.* **2000**, *3*, 35.
(7) Moens, L.; Vanfleteren, J.; van de Peer, Y.; Peeters, K.; Kapp, O.; Czeluzniak, J.; Goodman, M.; Blaxter, M.; Vinogradov, S. *Mol. Biol. Evol.* **1996**, *13*, 324.
(8) Pesce, A.; Couture, M.; Dewilde, S.; Guertin, M.; Yamauchi, K.; Ascenzi, P.; Moens, L.; Bolognesi, M. *EMBO J.* **2000**, *19*, 2424.
(9) Milani, M.; Pesce, A.; Nardini, M.; Ouellet, H.; Ouellet, Y.; Dewilde, S.; Bocedi, A.; Ascenzi, P.; Guertin, M.; Moens, L.; Friedman, J. M.; Wittenberg, J. B.; Bolognesi, M. *J. Inorg. Biochem.* **2005**, *99*, 97.
(10) Milani, M.; Pesce, A.; Ouellet, Y.; Ascenzi, P.; Guertin, M.; Bolognesi, M. *EMBO J.* **2001**, *20*, 3902.
(11) Milani, M.; Pesce, A.; Ouellet, Y.; Dewilde, S.; Friedman, J. M.; Ascenzi, P.; Guertin, M.; Bolognesi, M. *J. Biol. Chem.* **2004**, *279*, 21520.
(12) Crespo, A.; Martí, M. A.; Kalko, S. G.; Morreale, A.; Orozco, M.; Gelpí, J. L.; Luque, F. J.; Estrin, D. A. *J. Am. Chem. Soc.* **2005**, *127*, 4433.
(13) Bidon-Chanal, A.; Martí, M. A.; Crespo, A.; Milani, M.; Orozco, M.; Bolognesi, M.; Luque, F. J.; Estrin, D. A. *Proteins* **2006**, *64*, 457.

10.1021/ja0689987 CCC: $37.00

is mediated by three main structural features. First, the tunnel system would have evolved to allow access of O_2 and NO ligands to the heme through distinct migration paths. Second, O_2 binding to the heme would facilitate access of NO by promoting opening of the tunnel long branch, where ligand diffusion is controlled by PheE15, which acts as a gate. Third, opening of PheE15 would be mediated by a subtle conformational change in the hydrogen-bonded network formed by TyrB10 and GlnE11, which act as a molecular switch.

Since residues TyrB10 and GlnE11 are crucial to facilitate opening of the tunnel gate upon O_2 binding to the heme, disruption of the molecular switch should lead to a substantial decrease in the biological activity. In this study we examine the structural and dynamical properties of the TyrB10→Phe and GlnE11→Ala mutants in order to investigate the reliability of the dual-path ligand-induced regulation mechanism mentioned above. In particular, the results provide a molecular basis to explain the dramatic decrease in NO consumption observed experimentally for the TyrB10→Phe mutant and predict a similar behavior for the GlnE11→Ala mutant.

Methods

MD simulations were performed from the crystal structure of the oxygenated form of the wild type (wt) trHbN (PDB entry 1IDR; monomer A at 1.9 Å resolution),[9] which was used to generate the starting structures of the TyrB10→Phe and GlnE11→Ala mutants. This procedure is supported by the close similarity observed between the structure of the wt protein and the recently reported X-ray crystallographic structures of the cyanide complexes TyrB10→Phe and GlnE11→Ala mutants (PDB entries 2GKM and 2GLN).[14] As noted in ref 14, which also reports the X-ray structures of the GlnE11→Val (2GKN) and TyrB10→Phe/GlnE11→Val (2GL3) mutants, the rmsd of the A chain in the different mutants and in the wt protein ranges from 0.23 to 0.41 Å, thus confirming that the mutations have little impact on the protein fold. Every mutated enzyme was immersed in a preequilibrated octahedral box of TIP3P[15] water molecules. The standard protonation state at physiological pH was assigned to the ionizable residues. The final system contains the mutated protein, around 8600 water molecules, and the added counterions, leading to a total of ~28 300 atoms. Simulations were performed in the NPT ensemble.[16] The system was simulated employing periodic boundary conditions and Ewald sums (grid spacing of 1 Å) for treating long-range electrostatic interactions.[17] All simulations were performed with the parmm99 force field[18] using Amber8.[19] For the oxygenated heme group RESP charges[20] and HF/6-31G(d) wave functions were used according to the Amber standard protocol. The initial system was minimized and equilibrated using the multistep protocol reported for the wt protein.[12] Then, 100 ns MD simulation was run for the two mutants. As a reference control, a 50 ns MD simulation was performed for the oxygenated form of the wt trHbN using the same protocol.

The role of PheE15 as gate residue in the tunnel long branch was examined by computing classical molecular interaction potential (CMIP)[21] energy isocontour profiles using a rigid NO probe characterized by RESP atomic charges and van der Waals parameters defined for equivalent atoms in the Amber force field (see Supporting Information). To this end, the protein was placed in a grid (spacing of 0.35 Å) centered at the active site (heme group) and large enough to cover the whole channel.

The dynamical behavior of the proteins was investigated by determining the essential dynamics through principal component analysis,[22] conducted considering the backbone C_α atoms. Indeed, residues 1−15, which form the short N-terminal isolated helix, were excluded from the analysis since the high flexibility of this region might mask the essential movements in the trHbN fold. The similarity between essential motions for the wt protein and the mutants was quantified using the similarity index defined in eq 1, which takes into account not only the nature of the essential movements but also their contribution to the structural variance of the protein.[23]

$$\xi_{AB} = \frac{2\sum_{i=1}^{i=z}\sum_{j=1}^{j=z}\left\{(\nu_i^A\nu_j^B)\dfrac{\exp\left[-\dfrac{(\Delta x)^2}{\lambda_i^A}-\dfrac{(\Delta x)^2}{\lambda_j^B}\right]}{\sum_{i=1}^{i=z}\exp\left[-\dfrac{(\Delta x)^2}{\lambda_i^A}\right]\sum_{j=1}^{j=z}\exp\left[-\dfrac{(\Delta x)^2}{\lambda_i^B}\right]}\right\}}{\sum_{i=1}^{i=z}\left\{\dfrac{\exp\left[-2\dfrac{(\Delta x)^2}{\lambda_i^A}\right]}{\left(\sum_{i=1}^{i=z}\exp\left[-\dfrac{(\Delta x)^2}{\lambda_i^A}\right]\right)^2}\right\}+\sum_{j=1}^{j=z}\left\{\dfrac{\exp\left[-2\dfrac{(\Delta x)^2}{\lambda_i^B}\right]}{\left(\sum_{j=1}^{j=z}\exp\left[-\dfrac{(\Delta x)^2}{\lambda_i^B}\right]\right)^2}\right\}} \quad (1)$$

where λ_i is the eigenvalue associated with a given eigenvector i whose unitary vector is ν_i, and the sum is extended to a given set (z) of relevant eigenvectors.

Results and Discussion

To the best of our knowledge, there is no experimental evidence for the viability of the GlnE11→Ala mutant to accomplish the O_2/NO chemistry. However, Guertin and coworkers have shown that the TyrB10→Phe mutation leads to a drastic reduction in the NO-consuming activity compared to wt trHbN, since the NO consumption rate was similar to that measured in buffer solution,[2] which demonstrates that TyrB10 is essential for NO detoxification by trHbN. The decrease in the biological activity cannot be attributed to the inability of the TyrB10→Phe mutant to bind O_2. In fact, resonance Raman spectra confirm that it binds O_2, as noted in the Fe−O_2 stretching mode detected at 570 cm^{-1}.[24] Compared to the wt protein, however, the frequency of the Fe−O_2 stretching mode is shifted by around 10 cm^{-1} due to the loss of the hydrogen bond formed between the bound O_2 and the hydroxyl group of TyrB10 in trHbN.

On the basis of the preceding experimental evidence, one might be tempted to attribute the reduced activity of the TyrB10→Phe mutant to a loss in the catalytic efficiency of the

(14) Ouellet, Y.; Milani, M.; Couture, M.; Bolognesi, M.; Guertin, M. *Biochemistry* **2006**, *45*, 8770.
(15) Jorgensen, W. L.; Chandrasekhar, J.; Madura, J. D.; Impey, R. W.; Klein, M. L. *J. Chem. Phys.* **1983**, *79*, 926.
(16) Berendsen, H. J. C.; Postma, J. P. M.; van Gunsteren, W. F.; Di Nola, A.; Haak, J. R. *J. Chem. Phys.* **1984**, *81*, 3684.
(17) Darden, T. A.; York, D.; Pedersen, L. *J. Chem. Phys*. **1993**, *98*, 10089.
(18) Wang, J.; Cieplak, P.; Kollman, P. A. *J. Comput. Chem.* **2000**, *21*, 1049.
(19) Pearlman, D. A.; Case, D. A.; Caldwell, J. W.; Ross, W. R.; Cheatham, T. E., III; DeBolt, S.; Ferguson, D.; Seibel, G.; Kollman, P. *Comp. Phys. Commun.* **1995**, *91*, 1.
(20) Bayly, C. I.; Cieplak, P.; Cornell, W.; Kollman, P. A. *J. Phys. Chem.* **1993**, *97*, 10269.
(21) Gelpí, J. L.; Kalko, S.; de la Cruz, X.; Barril, X.; Cirera, J.; Luque, F. J.; Orozco, M. *Proteins* **2001**, *45*, 428.
(22) Amadei, A.; Linssen, A. B. M.; Berendsen, H. J. C. *Proteins* **1993**, *17*, 412.
(23) Meyer, T.; Ferrer-Costa, C.; Pérez, A.; Rueda, M.; Bidon-Chanal, A.; Luque, F. J.; Laughton, C. A.; Orozco, M. *J. Chem. Theory Comput.* **2006**, *1*, 251.
(24) Yeh, S. R.; Couture, M.; Ouellet, Y.; Guertin, M.; Rousseau, D. L. *J. Biol. Chem.* **2000**, *275*, 1679.

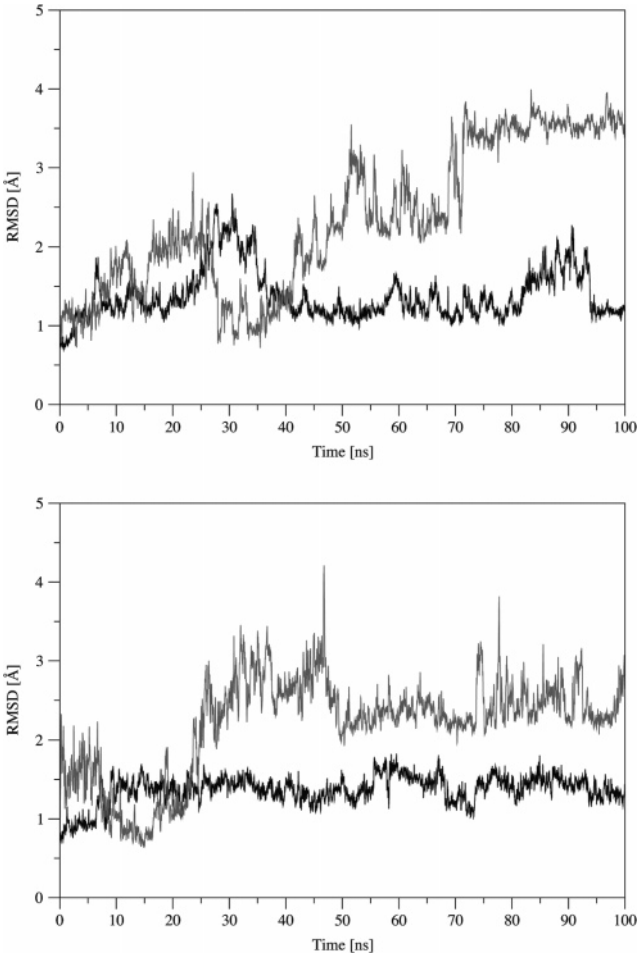

Figure 1. Positional root-mean-square deviation (Å) of the backbone atoms in the N-terminal (residues 1−15; gray) and core (residues 16−127; black) regions of the oxygenated forms of the TyrB10→Phe (top) and GlnE11→Ala (bottom) mutants determined relative to the X-ray structure of the wt protein (PDB entry 1IDR).

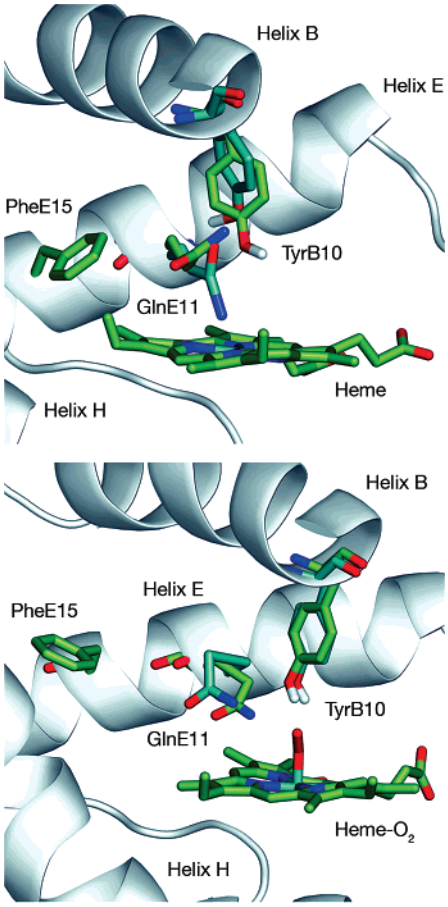

Figure 2. Hydrogen-bonded interactions between TyrB10 and GlnE11 in trHbN and trHbN•O_2 forms. (Top) In the deoxygenated form the side chain of GlnE11 adopts an *all-trans* conformation (average torsions around $C_\alpha-C_\beta$, $C_\beta-C_\gamma$, and $C_\gamma-C_\delta$ dihedrals of 40.2°, 167.1°, and 93.7°), and the relative orientation of the amide group of GlnE11 and the hydroxyl group of TyrB10 fluctuates along the trajectory, so that the GlnE11 amide acts as either donor (NH_2) or acceptor (C═O) in the hydrogen bond formed with TyrB10. (Bottom) In trHbN•O_2 the heme-bound O_2 is hydrogen-bonded to the TyrB10 OH group, which forces the GlnE11 amide to act only as hydrogen-bond donor. To this end, the side chain of GlnE11 populates two *staggered* conformations (average torsional angles around $C_\alpha-C_\beta$, $C_\beta-C_\gamma$, and $C_\gamma-C_\delta$ bonds of 45.0°, −74.8°, −99.3° and −50.2°, 67.2°, 48.5°, respectively). The conformational change of PheE15 leading to opening/closing of the tunnel long branch is illustrated by comparison of the structures (top: closed state; bottom: open state).

protein in the conversion of NO to nitrate anion. However, our previous studies of the chemical reaction in the wt protein and in the TyrB10→Phe mutant suggest that the replacement of Tyr by Phe does not exert a significant influence on the energetics of the reaction.[11] Then, it is unclear why the TyrB10→Phe mutant, which can bind O_2 and can accomplish the NO chemical conversion to nitrate anion, has an extremely low efficiency. It can be speculated that the low NO consumption of the TyrB10→Phe mutant stems from the disruption of the molecular mechanism that assists ligand diffusion to the O_2-bound heme, which presumably involves the TyrB10−GlnE11 pair. Analogously, it can be hypothesized that mutation of GlnE11 to Ala should also disrupt such a ligand migration mechanism.

MD Simulations of the oxy TyrB10→Phe and GlnE11→Ala Mutants. To explore the reliability of the preceding hypothesis, 100 ns MD simulations of the oxygenated form of the TyrB10→Phe and GlnE11→Ala mutants were performed. In the two cases stable trajectories, without large structural fluctuations, were obtained (rmsd for core residues (16−127) around 1.5 Å). The only noticeable displacements were found in the pre-helix A in the N-terminal region (rmsd for residues 1−15 in the range 2−3.5 Å; see Figure 1). Note that the same behavior was obtained in previous simulations of wt trHbN•O_2.[11]

Our previous studies[11,12] pointed out that PheE15 acts as the gate of the tunnel long branch in the wt trHbN•O_2, thus supporting the original proposal about the gating role of this residue made by Milani et al.[10] In fact, PheE15 populates two main conformations characterized by average $C_\alpha-C_\beta$ torsional angles of about +40° and −50° (see Figure 2; those dihedral angles, which are defined relative to the $H_\alpha-C_\alpha-C_\beta-C_\gamma$ torsion, would be around −80° and 170° when the $N-C_\alpha-C_\beta-C_\gamma$ torsion is used). In the former, the phenyl ring protrudes into the tunnel branch, thus preventing access of incoming ligands to the heme distal cavity (*closed* state), but in the latter the benzene ring is roughly parallel to the axis of the tunnel, which enables the transit of diatomic ligands (*open* state). In fact, these conformational states are reflected in two distinct conformations observed for PheE15 in the X-ray crystallographic structure of the wt protein (unit A in the PDB entry 1IDR, where the $N-C_\alpha-C_\beta-C_\gamma$ torsional angle adopts values close to −91° and −155°, respectively, for the closed and open states).

The analysis of the 50 ns MD simulation of the wt trHbN•O_2 supported the ability of PheE15 to populate the two conforma-

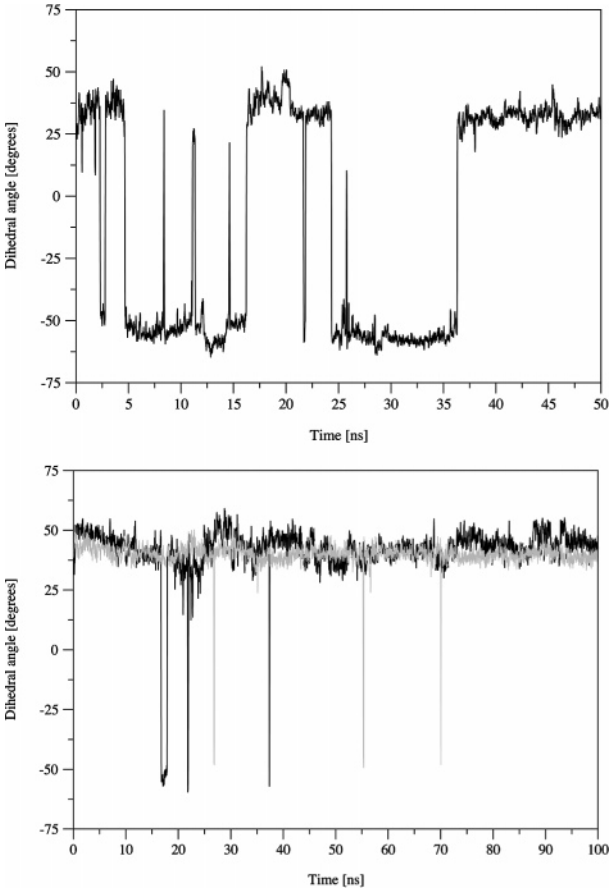

Figure 3. Time-dependence conformation of the torsional angle (deg) around the $C_\alpha-C_\beta$ bond of PheE15 along trajectories sampled for the oxygenated form of (top) the wt trHbN and (bottom) their TyrB10→Phe (black) and GlnE11→Ala (gray) mutants. The torsional angle $H_\alpha-C_\alpha-C_\beta-C_\gamma$ is used to follow the conformational fluctuations of PheE15. Note the different length of the MD simulations for the wt protein (50 ns) and the mutants (100 ns).

tional states. As noted in Figure 3, the trajectory reveals the occurrence of several transitions between *open* and *closed* states, the population of the *open* state being close to 53% (Figure 3). In fact, the analysis allowed us to identify the migration of a water molecule through the tunnel long branch, which transiently remained in the distal side of the heme pocket before being released to the bulk solvent. In contrast, the PheE15 conformational behavior observed for TyrB10→Phe and GlnE11→Ala mutants is drastically different. Thus, not only was a lower number of transitions between *open* and *closed* states detected (Figure 3), but the population of the *open* state was found to be negligible. In fact, PheE15 adopted a conformation defined by an average $C_\alpha-C_\beta$ ($H_\alpha-C_\alpha-C_\beta-C_\gamma$) torsional angle of about $+40°$ in the two mutants, which would impede migration of NO through the long channel (no water molecule was found to migrate along the tunnel even though the length of the MD simulations of the mutants was twice that used for the wt protein).

The blockade of the tunnel in the *closed* conformation of the PheE15 gate for the two mutants was supported by the CMIP isocontour plots for the interaction of a NO probe with the wt protein and their mutants. For a series of snapshots taken regularly along the trajectory, a favorable interaction energy region was identified in the distal side of the heme group (see Figure 4). Such a region protudes toward the intersection of

Figure 4. Classical molecular interaction potential isocontour plots determined for the interaction with a NO probe particle for the oxygenated form of the wt trHbN (top) and their TyrB10→Phe (middle) and GlnE11→Ala (bottom) mutants. The gate residue PheE15 obtained from five representative snapshots is also shown. The spheres stand for the heme iron and the bonded O_2 molecule.

the two tunnel branches, thus occupying a space in the cavity that coincides with one of the secondary Xe binding sites recently identified by Bolognesi's group upon treatment of trHbN crystals under Xe pressure.[10] For the mutants, however, the energy isocontour along the tunnel long branch is broken due to the presence of the PheE15 benzene ring (Figure 4, middle and bottom). In this case, the favorable interaction energy located near the benzene ring, but in the outer part of the tunnel, agrees with the main Xe binding site identified by Bolognesi et al.[10] In constrast, the CMIP isocontour determined for the

wt trHbN•O_2 (Figure 4, top) clearly delineates an energetically favorable path leading from the outer space to the heme cavity.

Essential Dynamics of the TyrB10→Phe and GlnE11→Ala Mutants. The preceding findings point out that the conformational flexibility of PheE15 is severely restricted in the oxy form of both TyrB10→Phe and GlnE11→Ala mutants. In trHbN•O_2 the transition between *open* and *closed* states of PheE15 is regulated by a salt bridge between Arg10 (in the N-terminal region) and Glu70 (in the EF interhelical region). This salt bridge is formed upon folding of the short A helix onto the EF hinge, which increases the friction between helices B and E, thus inhibiting opening of the tunnel long branch. The Arg10−Glu70 salt bridge is not observed in the X-ray crystallographic structure of the wt protein, even though this might simply stem from crystal packing. On the other hand, the physiological role of the pre-A region in trHbN remains unknown, thus making it necessary to be cautious in attributing a functional role to such an interaction. In any case, a similar folding effect might also justify the conformational restriction of Phe15 observed in the two mutants. However, the analysis of the whole trajectory revealed that this is not the case, since the salt bridge is not formed (the distance between Arg10 and Glu70 was in general larger than 20 Å; see Supporting Information). These findings, therefore, suggest that the reduced conformational flexibility of PheE15 must stem from the intrinsic inability of the mutant to induce the opening of the channel upon O_2 binding.

Our previous studies for wt trHbN•O_2 suggested that O_2 binding to the heme introduces a major change in the protein essential dynamics, which favors opening of the tunnel long branch by enhancing the relative displacement of helices B and E.[12] The essential dynamics analysis of the oxygenated forms of TyrB10→Phe and GlnE11→Ala mutants revealed a drastic difference in the natural movements of the protein backbone compared to the wt trHbN•O_2. Thus, the main contributions to the backbone structural fluctuations stems from helices G and H and the loop F in the TyrB10→Phe mutant (Figure 5, top) and from helices C, G, and H in the GlnE11→Ala mutant (Figure 5, bottom).

The difference in the main structural fluctuations of trHbN•O_2 and the two mutants can be measured by means of the similarity index ξ_{AB} (see eq 1 in Methods),[24] which takes into account not only the nature of the essential movements but also their contribution to the structural variance of the protein. Thus, for the 10 most relevant essential motions of the backbone skeleton in the core region of wt trHbN•O_2 and TyrB10→Phe•O_2, which account for around 70% of the structural variance, the similarity index only amounts to 0.48, which is clearly smaller than the self-similarities obtained for the wt protein and the TyrB10→Phe mutant (0.74 and 0.86, respectively; see Supporting Information). Interestingly, when such an analysis is performed separately for the pair of helices G−H, the similarity index is 0.45, whereas it only amounts to 0.26 for the pair of helices B−E. This indicates that the dynamical behavior of these two helices is highly different in wt trHbN•O_2 and the TyrB10→Phe•O_2 mutant.

Similar findings are obtained from the comparison of the essential dynamics of wt trHbN•O_2 and the GlnE11→Ala•O_2 mutant. In this case, the global similarity index (0.37, which compares with self-similarities of 0.74 and 0.89 for the wt and the GlnE11→Ala mutant; see Supporting Information) is larger than that obtained separately for helices B−E (0.30), but lower than that determined for the motion of helices G−H (0.52). Overall, these findings reveal the different nature of the motions in the wt protein and in the two mutants and particularly the disappearance of the relative displacement observed between helices B and E in wt trHbN•O_2, which is lost in the two mutants.

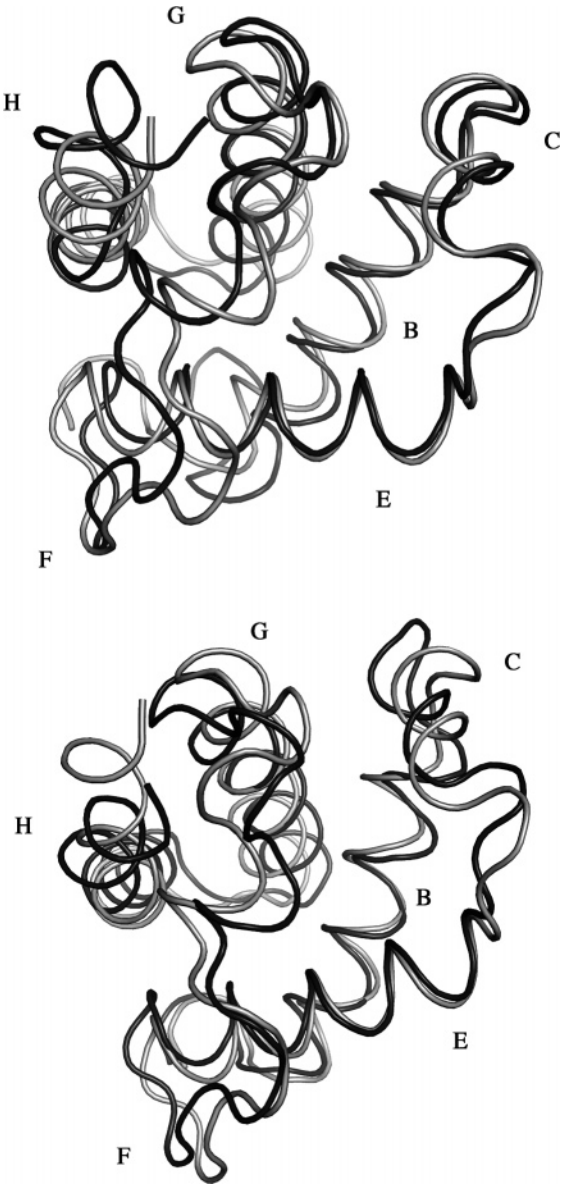

Figure 5. Representation of the backbone structural fluctuations due to essential dynamics motions in the oxygenated forms of TyrB10→Phe (top) and GlnE11→Ala (bottom) mutants. Structures in black and gray illustrate the regions in the peptide skeleton mostly affected by the essential movements (the labels denote the structural elements in trHbN).

Dynamical Behavior of the TyrB10(Phe) and GlnE11(Ala) Residues. The alteration in the essential dynamics of the protein backbone induced in trHbN upon O_2 binding to the heme is assisted by the hydrogen-bonded TyrB10−GlnE11 pair, which acts as a molecular switch.[12] In the deoxygenated trHbN, GlnE11 adopts an extended *all-trans* conformation, allowing the terminal amido group to be hydrogen-bonded to the hydroxyl group of TyrB10. In fact, there is a dynamical fluctuation between (TyrB10)O−H···O═C(GlnE11) and (TyrB10)O···H−N(GlnE11) hydrogen bonds, so that the hydroxyl group of TyrB10 acts as both hydrogen-bond donor and acceptor (Figure 2, top).

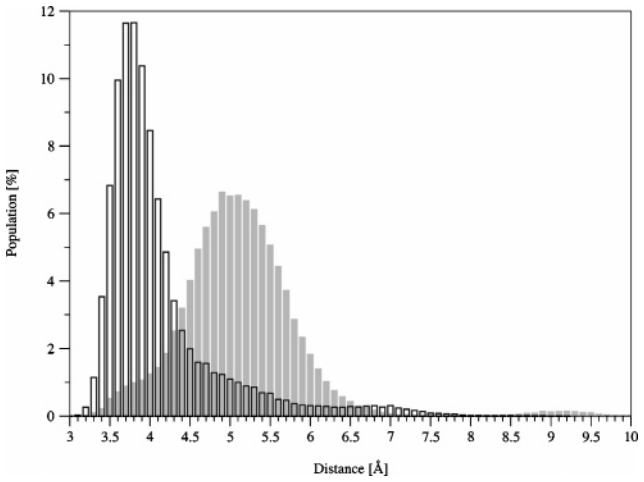

Figure 6. Distribution of interesidue distances between the side chains of GlnE11 and PheE15 in the oxygenated forms of the wt protein (white bars) and its TyrB10→Phe mutant (gray bars).

In contrast, since the heme-coordinated O_2 fixes TyrB10 through a hydrogen bond in trHbN·O_2, the TyrB10 hydroxyl group acts exclusively as hydrogen-bond acceptor for the amide NH_2 group of GlnE11, whose side chain populates two *staggered* conformations (Figure 2, bottom).

The transition between extended and staggered conformations of GlnE11 is associated with a notable variation in the separation between the side chains of GlnE11 and PheE15 (see Figure 6). The distance from the side chain of GlnE11 to the PheE15 benzene ring in trHbN·O_2 is, on average, close to 3.9 Å, but the contacts between the side chains of GlnE11 and PheE15 can be as short as 3.1 Å (Figure 6). In fact, there is a sizable fraction of structures (around 45%) having a separation contact below 3.9 Å (i.e., the van der Waals contact between $-CH_2-$ and $>CH$ groups according to Pauling's radii). In contrast, in the deoxygenated form of trHbN, where GlnE11 adopts an extended conformation (see above), the average distance between GlnE11 and PheE15 is enlarged by around 1.5 Å. Therefore, it can be concluded that the alteration of the hydrogen-bonded interaction in the TyrB10−GlnE11 pair induced upon O_2 binding to the heme triggers a compression mechanism onto the benzene ring of PheE15, which is proposed to favor opening of the gate in the tunnel long branch.

The molecular switch formed by TyrB10−GlnE11 is greatly affected by the two mutations examined here. In the TyrB10→Phe mutant, GlnE11 forms a hydrogen-bond interaction with the heme-bound O_2. Such an interaction is maintained along the whole trajectory (average N···O distance of 3.0 Å) and forces GlnE11 to adopt an *all-trans* conformation. Inspection of the X-ray crystallographic structure of the cyanide complex of the TyrB10→Phe mutant[14] shows that GlnE11 also forms a hydrogen bond with the cyanide ligand. However, in the X-ray structure GlnE11 adopts a *staggered* conformation. This conformational difference can be mainly attributed to the different tilt of the two ligands, as noted in the angles formed by the diatomic molecules and the heme iron (values averaged for units A and B of 118.3° (Fe···O_2) and 168.3° (Fe···CN) in 1IDR and 2GKM, respectively), though it can also be affected, at least in part, by the steric hindrance due to PheB10, since the shortest contact between the carbon atoms in the benzene ring and the cyanide unit is 3.2 Å in the X-ray structure, which is around 1 Å lower than the average separation found in the MD simulation.

The direct interaction formed between GlnE11 and heme-bound O_2 makes the separation of the side chains of GlnE11 and PheE15 amount, on average, to 5.2 Å, which is notably larger than that found for the oxygenated wt protein (Figure 6). As a result, the conformational compression mechanism operative in wt trHbN·O_2 is completely lost in the TyrB10→Phe mutant, as noted in the fact that the population of structures with a separation between the side chains of GlnE11 and PheE15 lower than 3.9 Å is less than 4%. This effect, combined with the increased friction between helices B and E, should reduce the opening of the PheE15 gate.

In the case of the GlnE11→Ala mutant, where TyrB10 remains hydrogen-bonded to the heme-bound O_2 molecule (average O···O distance of 2.8 Å), the reduction in size and hydrogen-bond capability that accompanies the replacement of GlnE11 by Ala breaks the molecular switch that triggers opening of the PheE15 gate.

Functional Implications. The reduced catalytic activity observed for the TyrB10→Phe mutant can be ascribed to the inability of the PheB10−GlnE11 pair to trigger the local conformational change leading to (i) an increase in the local compression mechanism exerted by GlnE11 onto the side chain of PheE15 and (ii) the change in the global essential dynamics of the protein, which should favor the relative displacement of helices B and E. The ligand-induced regulation of the global structural plasticity of the protein is supported by experimental data indicating that NO-binding to the ferric heme group of the trHbN promotes a large-scale conformational change in the protein that propagates through the pre-F helix to the E and B helices.[25] Further support comes from the experimentally observed dependence of the kinetics of ligand diffusion in trHbN on the viscosity of the aqueous environment,[26] which suggests that the dynamical behavior of the protein is directly implicated in the regulation of ligand migration. In fact, the involvement of different conformational states in the dynamical modulation of ligand migration is also indicated by the different kinetic pattern observed in CO recombination assays in trHbN and its TyrB10→Phe mutant.[27]

Whereas the inability of the TyrB10→Phe mutant to capture NO can be ascribed to the direct hydrogen-bond interaction formed between GlnE11 and heme-bound O_2, which impedes the occurrence of the *local* conformational changes detected in the TyrB10−GlnE11 pair for the wt protein, our results also indicate that the oxygenated form of the GlnE11→Ala mutant should be inactive against NO consumption. In this case, despite the larger size of the heme pocket arising from the replacement of GlnE11 by Ala, the lack of NO-consumption activity should be attributed to the inability of Ala to compress *locally* the gate (PheE15) of the tunnel long branch and to promote the *global* change in the essential dynamics leading to motion of helices B and E.

On the basis of the preceding results, it can be concluded that the TyrB10−GlnE11 pair, besides their contribution to the high oxygen affinity of the protein (O_2-binding affinity to ferrous

(25) Mukai, M.; Ouellet, Y.; Guertin, M.; Yeh, S.-R. *Biochemistry* **2004**, *43*, 2764.
(26) Dantsker, D.; Samuni, U.; Ouellet, Y.; Wittenberg, B. A.; Wittenberg, J. B.; Milani, M.; Bolognesi, M.; Guertin, M.; Friedman, J. M. *J. Biol. Chem.* **2004**, *279*, 38844.
(27) Samuni, U.; Dantsker, D.; Ray, A.; Wittenberg, J. B.; Wittenberg, B. A.; Dewilde, S.; Moens, L.; Ouellet, Y.; Guertin, M.; Friedman, J. M. *J. Biol. Chem.* **2003**, *278*, 27241.

trHbN of 8.0×10^{-9} with a k_{off} of 0.2 s^{-1})[8] and to the correct positioning of the incoming NO ligand in the O_2-bound heme cavity, acts as a molecular switch that regulates opening of the tunnel long branch and facilitates ligand (NO) migration to the O_2-bound heme. In fact, since the NO conversion to nitrate by trHbN•O_2 occurs at a rate faster than O_2 binding to the deoxy protein (the bimolecular rate constants for these two processes are 745 and 25 μM^{-1} s^{-1}, respectively),[2,8] this role might be considered to be the most critical factor to warrant survival of *M. tuberculosis* under stress conditions.

Finally, in line with previous studies carried out to identify the factors that modulate ligand migration in heme proteins,[28−32] these results point out that the dual-path ligand-induced dynamical regulation mechanism in trHbN relies on a small number of key residues. This finding opens challenging questions relative to the involvement of similar ligand diffusion mechanisms in other truncated hemoglobins, whose activity might be regulated by motional fluctuations of certain structural domains[33] or even in the recently discovered neuroglobin and cytoglobin.[34−36] A particularly challenging case is trHbN of *M. smegmatis*, which has nearly 70% sequence similarity with trHbN of *M. tuberculosis* and retains most of the structural features crucial to attain the trHb fold.[37] In fact, PheE15, TyrB10, and GlnE11 are retained, and the protein binds oxygen reversibly with high affinity. Nevertheless, the NO-metabolizing activity of *M. smegmatis* trHbN is significantly lower than that of the *M. tuberculosis* protein.[37] It is not clear whether this functional difference might come from the lack of the highly polar and charged N-terminal sequence motif that constitutes the pre-A region in *M. tuberculosis* trHbN. Present results allow us to speculate that such a functional difference might also stem from an alteration in the dynamical behavior of the protein skeleton, which might affect the regulation mechanism that facilitates NO diffusion through the protein matrix. Clearly, untangling the structural basis of the interplay between ligand binding, protein dynamics, and ligand migration will shed light on the emerging field of multiligand chemistry in heme proteins.

Acknowledgment. We are grateful to Prof. M. Orozco for valuable discussions and suggestions. This work was partially supported by grants from Universidad de Buenos Aires (grant X038), ANPCYT (grant 25667), and the Spanish Ministerio de Educación y Ciencia (grant CTQ2005-08797-C02-01/BQU). Calculations were performed in the MareNostrum supercomputer at the Barcelona Supercomputing Center. Contribution dedicated to the memory of Prof. L. Pueyo.

Supporting Information Available: Parameters of the NO rigid probe used in CMIP computations. Plots for the probability distribution of the $C_\alpha-C_\beta$ dihedral angle of PheE15, and time dependence of the distance between Arg10 and Glu70. Tables reporting similarity indexes for the most relevant motions of the backbone and selected helices. This material is available free of charge via the Internet at http://pubs.acs.org.

JA0689987

(28) Schotte, F.; Lim, M.; Jackson, T. A.; Smirnov, A. V.; Soman, J.; Olson, J. S.; Phillips, G. N., Jr.; Wulff, M.; Anfinrud, P. A. *Science* **2003**, *300*, 1944.
(29) Chu, K.; Vojtchovský, J.; McMahon, B. H.; Sweet, R. M.; Berendzen, J.; Schlichting, I. *Nature* **2000**, *403*, 921.
(30) Case, D. A.; Karplus, M. *J. Mol. Biol.* **1979**, *132*, 343.
(31) Bossa, C.; Anselmi, M.; Roccatano, D.; Amadei, A.; Vallone, B.; Brunori, M.; Di Nola, A. *Biophys. J.* **2004**, *86*, 3855.
(32) Nutt, D. R.; Meuwly, M. *Proc. Natl. Acad. Sci. U.S.A.* **2004**, *101*, 5998.
(33) Marsella, L. *Proteins* **2006**, *62*, 173.
(34) Ascenzi, P.; Salvati, L.; Brunori, M. *FEBS Lett.* **2001**, *501*, 103.
(35) Eich, R, F.; Li, T.; Lemon, D. D.; Doherty, D. H.; Curry, S. R.; Aitken, J. F.; Mathews, A. J.; Johnson, K. A.; Smith, R. D.; Phillips, G. N., Jr.; Olson, J. S. *Biochemistry* **1996**, *35*, 6976.
(36) Brunori, M.; Giuffrè, A.; Nienhaus, K.; Nienhaus, G. U.; Scandurra, F. M.; Vallone, B. *Proc. Natl. Acad. Sci. U.S.A.* **2005**, *102*, 8483.
(37) Lama, A.; Pawaria, S.; Dikshit, K. L. *FEBS Lett.* **2006**, *580*, 4031.